

# Chiral Extrapolation of Lattice Data for Heavy Meson Hyperfine Splittings

X.-H. Guo<sup>1,2,\*</sup>, P. C. Tandy<sup>3,\*\*</sup>, A. W. Thomas<sup>4,\*\*\*</sup>

<sup>1</sup> Key Laboratory of Radiation Beam Technology and Material Modification of National Ministry of Education, and Institute of Low Energy Nuclear Physics, Beijing Normal University, Beijing 100875, China

<sup>2</sup> Department of Physics and Mathematical Physics, and Special Research Center for the Subatomic Structure of Matter, Adelaide University, SA 5005, Australia

<sup>3</sup> Center for Nuclear Research, Department of Physics, Kent State University, Kent, Ohio 44242, USA

<sup>4</sup> Jefferson Lab, 12000 Jefferson Avenue, Newport News, VA 23606, USA

**Abstract.** We investigate the chiral extrapolation of the lattice data for the light-heavy meson hyperfine splittings  $D^* - D$  and  $B^* - B$  to the physical region for the light quark mass. The chiral loop corrections providing non-analytic behavior in  $m_\pi$  are consistent with chiral perturbation theory for heavy mesons. Since chiral loop corrections tend to decrease the already too low splittings obtained from linear extrapolation, we investigate two models to guide the form of the analytic background behavior: the constituent quark potential model, and the covariant model of QCD based on the ladder-rainbow truncation of the Dyson-Schwinger equations. The extrapolated hyperfine splittings remain clearly below the experimental values even allowing for the model dependence in the description of the analytic background.

## 1 Introduction

In the past few years there has been much progress in lattice gauge theory with many physical quantities having been calculated. Among them the hyperfine splittings in the heavy meson systems are of particular interest. With the aid of nonrelativistic QCD (NRQCD) on the lattice, the authors of Ref. [1] reported three lattice data for the  $qQ$  meson hyperfine splittings  $D^* - D$  and  $B^* - B$ . These data were obtained in the unphysical region where  $m_q$  corresponds to  $m_\pi$  being larger than about 680 MeV. With a naive linear extrapolation to the physical  $m_\pi$ , the extrapolated hyperfine splittings are typically 120 MeV for  $D^* - D$ , and

\* *E-mail address:* xhguo@bnu.edu.cn

\*\* *E-mail address:* tandyc@cnr2.kent.edu

\*\*\* *E-mail address:* awthomas@jlab.org

32 MeV for  $B^* - B$ . These are significantly smaller than the experimental values 140 MeV and 46 MeV respectively. The obvious shortcoming in the naive linear extrapolation is that the nonanalytic terms in the light quark mass, generated by chiral loops, do not appear.

To correct this, we previously [2, 3] included pion loop contributions by applying heavy meson chiral perturbation theory at small  $m_\pi$ , following a series of works in this direction [4]. This leads to rapid, nonanalytic variation when  $m_\pi$  is smaller than about 400 - 500 MeV (which corresponds to a current quark mass  $m_q \sim 60$  MeV). When  $m_\pi$  is larger than 400 - 500 MeV, the heavy meson mass varies slowly and smoothly and is linear in  $m_\pi^2$ , as indicated by the lattice data. Such considerations of the behavior of the individual meson masses led to the suggestion that the hyperfine splitting,  $y_P = m_{P^*} - m_P$ , for the heavy meson,  $P$ , can be extrapolated with the following form:

$$y_P = \bar{\sigma}_P + a_P + b_P m_\pi^2, \quad (1)$$

where  $\bar{\sigma}_P \equiv \sigma_{P^*} - \sigma_P$ , and  $\sigma_{P(P^*)}$  the pion loop contribution to the meson mass of  $P$  ( $P^*$ ). This guarantees the correct chiral limit behavior, and  $a_P$  and  $b_P$  are fit parameters. The resulting extrapolated values for the hyperfine splittings for both  $D$  and  $B$  mesons are even smaller than those obtained in the naive linear extrapolation [2, 3].

Here we investigate the appropriateness of the last two terms of Eq. (1) in representing the “analytic background” physics to which the chiral loop contributions are added. We investigate the constraints from two models: the constituent quark potential model (CQM), and the Dyson-Schwinger equation (DSE) model in ladder-rainbow truncation [5]. For all the hadron properties which have been calculated in lattice QCD, the lattice results vary slowly and smoothly when  $m_q$  is larger than about 60 MeV. This is characteristic of constituent quark behavior [6] and suggests the use of the constituent quark mass for an efficient description of hadron properties in this region. The CQM emphasizes such a concept.

On the other hand, the DSE ladder-rainbow model is a covariant modeling of QCD that satisfies the chiral symmetry constraints. In particular, it properly incorporates dynamical chiral symmetry breaking [7] which plays a dominant role in hyperfine splitting of physical ground states [8, 9]. No explicit chiral loops are present at ladder-rainbow truncation; nevertheless the relation between pseudoscalar mass and quark current mass has the correct leading behavior at low and high quark mass [10].

An analytic background form for hyperfine splitting is deduced from the CQM in Sec. 2, and from the DSE model in Sec. 3 and comparisons are made there. The chiral loop contributions to the hyperfine splitting are discussed in Sec. 4, and the chirally extrapolated results are presented in Sec. 5. A summary is made in Sec. 6.

## 2 Constituent Quark Potential Model

The constituent quark model (CQM) has been shown to work quite well even though it is a very simple model which has not been derived from Quantum

Chromodynamics. The constituent quark mass,  $M_q$  (where  $q$  denotes a  $u$  or  $d$  quark), is linked to the current quark mass,  $m_q$ , in the following way [6]:

$$M_q = M_\chi + c m_q, \quad (2)$$

where  $c$  is of order 1 and  $M_\chi$  is the constituent quark mass in the chiral limit which originates from dynamical chiral symmetry breaking in QCD.

In the constituent quark potential model, the potential between a quark and an antiquark consists of scalar and vector parts. The hyperfine splitting is caused by the relativistic spin-spin interaction between the quark and the antiquark. We consider the model where the vector part of the potential is caused by one-gluon-exchange. Then the hyperfine splitting for the heavy meson  $\bar{Q}q$  is [11]

$$y_P^{\text{CQM}} = \frac{32}{9}\pi\alpha_s \frac{1}{M_Q M_q} |\psi(0)|^2, \quad (3)$$

where  $M_Q$  is the constituent quark mass of the heavy quark  $Q$ ,  $\alpha_s$  is the strong coupling constant, and  $\psi(0)$  is the wave function of the heavy meson at the origin. On the other hand,  $\psi(0)$  can be expressed as [11]:  $|\psi(0)|^2 = \frac{1}{2\pi} \frac{M_Q M_q}{M_Q + M_q} \langle V'(r) \rangle$ . In a heavy meson which consists of a light quark and a heavy antiquark the dynamics is mainly determined by the light degrees of freedom due to heavy quark symmetry. The long distance part of  $V(r)$  is the most relevant, and for a typical potential model with linear confinement,  $\langle V'(r) \rangle$  is essentially independent of quark masses. Consequently, from the CQM we expect the mass dependence of hyperfine splitting to be well-represented by

$$y_P^{\text{CQM}} = \frac{\tilde{d}_P}{M_q + M_Q}, \quad (4)$$

where  $\tilde{d}_P$  is a constant.

The constituent quark mass  $M_q$  in Eq. (4) will vary with  $m_\pi^2$  because of Eq. (2) and the variation of current mass  $m_q$  with  $m_\pi^2$  due to chiral symmetry. The latter variation we take from the Gell-Mann–Oakes–Renner (GMOR) relation in the form:  $\frac{m_q}{m_q^{\text{phys}}} = \frac{m_\pi^2}{(m_\pi^{\text{phys}})^2}$ , where  $m_q^{\text{phys}}$  is the quark mass associated with the physical pion mass,  $m_\pi^{\text{phys}}$ . Lattice studies indicate this relation is acceptable up to  $m_\pi \sim 1$  GeV. Then with Eq. (2) one has  $M_q = M_\chi + \frac{c m_q^{\text{phys}}}{(m_\pi^{\text{phys}})^2} m_\pi^2$  [6], and Eq. (4) takes the more convenient form

$$y_P^{\text{CQM}} = \frac{d_P}{e_P + m_\pi^2}. \quad (5)$$

Here  $d_P \equiv \tilde{d}_P \frac{(m_\pi^{\text{phys}})^2}{c m_q^{\text{phys}}}$  and  $e_P \equiv e' + M_Q \frac{(m_\pi^{\text{phys}})^2}{c m_q^{\text{phys}}}$  with  $e'$  being defined as  $M_\chi \frac{(m_\pi^{\text{phys}})^2}{c m_q^{\text{phys}}}$ .

We expect  $y_P^{\text{CQM}}$  to be a better representation of the ‘‘analytic background’’ physics than the last two terms of Eq. (1) for several reasons. Firstly, while  $y_P^{\text{CQM}}$  shares with the background part of Eq. (1) a linear behavior with small

$m_\pi^2$ , its dependence on  $M_Q$  is consistent with heavy quark effective theory [12]. In contrast, Eq. (1) provides no explicit  $M_Q$  dependence. Secondly, the two parameters of Eq. (1) are totally phenomenological while the parameter  $e_P$  of  $y_P^{\text{CQM}}$  is constrained by existing applications of the CQM to other baryon physics. For example, the ratio of the constituent quark masses of the strange quark and the  $u, d$  quark is given by  $\frac{M_s}{M_{u,d}} = \frac{e' + (m_\pi^2)_s}{e' + (m_\pi^{\text{phys}})^2}$ , where  $(m_\pi^2)_s$  is the pion mass squared when  $m_q$  is equal to  $m_s$ . Use of the CQM and chiral perturbation theory to guide the extrapolation of the magnetic moments of the spin-1/2 baryon octet leads to  $M_s/M_{u,d} \sim 1.3$  [6]. We let this ratio vary between 1.2 and 1.4. Use of the GMOR relation between  $m_\pi^2$  and  $m_q$  leads to  $(m_\pi^2)_s \sim 0.5 \text{ GeV}^2$ . Consequently we allow the range of  $e'$  to be from 1.2  $\text{GeV}^2$  to 2.5  $\text{GeV}^2$ . The CQM fit in Ref. [6] found  $c m_q^{\text{phys}} \sim 5.90 \text{ MeV}$ . If we take the heavy constituent masses to be  $M_c \sim 1.3 - 1.7 \text{ GeV}$  and  $M_b \sim 4.6 - 5.0 \text{ GeV}$ , then we have the parameter ranges  $e_D \sim 5.5 - 8.2 \text{ GeV}^2$  and  $e_B \sim 16.5 - 19.2 \text{ GeV}^2$ .

In Sec. 5 we add the pion loop contribution to  $y_P^{\text{CQM}}$  and fit the single free parameter  $d_P$  to the lattice data, while constraining  $e_P$  to be within the above expected range. For the sake of comparison, the  $m_\pi^2$  dependence from  $y_P^{\text{CQM}}$  alone is illustrated here by a preliminary fit of  $y_P^{\text{CQM}}$  to the lattice data, allowing both  $d_P$  and  $e_P$  to vary freely. This is displayed in Figs. 1 and 2. (The meaning of the model denoted CQM' in those figures is explained in the next Section.) We obtain  $d_D = 0.547 \text{ GeV}^3$ ,  $e_D = 4.462 \text{ GeV}^2$ , and  $d_B = 0.447 \text{ GeV}^3$ ,  $e_B = 14.71 \text{ GeV}^2$  for  $y_D^{\text{CQM}}$  and  $y_B^{\text{CQM}}$  respectively. These  $e_P$  values are just below the expected range.

### 3 Dyson-Schwinger Equation Model

Information on hyperfine splitting in the absence of chiral loops can also be obtained from the modeling of mesons through the Dyson-Schwinger equations (DSE) of QCD in rainbow-ladder truncation [14, 9]. This a Poincaré covariant approach that implements the correct one-loop renormalization group behavior of QCD [13] and the relevant Ward–Takahashi identities. The resulting axial current conservation preserves the Goldstone nature of the pseudoscalars [7]. With one infrared parameter (besides the quark current masses) the model [14] provides an efficient description of the masses and decay constants of the light-quark pseudoscalar and vector mesons [13, 14], the elastic charge form factors  $F_\pi(Q^2)$  and  $F_K(Q^2)$  [15] and the electroweak transition form factors of the pseudoscalars and vectors [16, 17].

The current quark mass dependence of the DSE results satisfies the exact QCD pseudoscalar mass relation [7]. For  $qQ$  mesons it takes the form [7]  $m_P^2 f_P = (m_q + m_Q) R_P$  where the electroweak decay constant  $f_P$ , and the projection  $R_P$  of the Bethe-Salpeter wave function onto  $\gamma_5$  at the origin of  $\bar{q}q$  separation, are dependent upon the current masses  $m_q$  and  $m_Q$ . The quark masses and  $R_P$  are dependent upon renormalization scale  $\mu$  but the mass relation is not. The chiral limit of  $R_P$  is [7]  $R_{P,\mu}^0 = -\langle \bar{q}q \rangle_\mu / f_P^0$ , where  $f_P^0$  is the chiral limit value; thus the GMOR relation follows as a corollary of the exact relation in the low mass limit. [The error in the GMOR relation at the  $K$  meson is 4%, at  $m_Q = 0.4 \text{ GeV}$  the

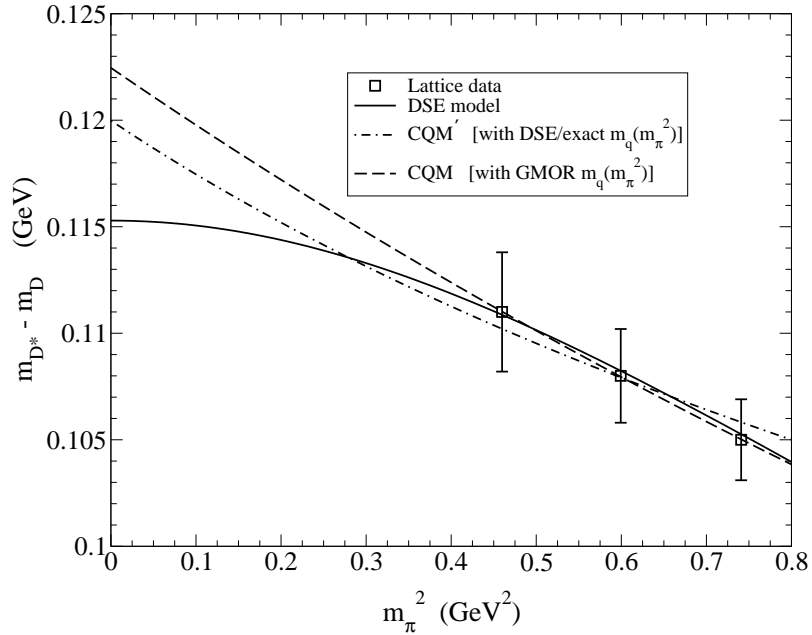


**Figure 1.** The “analytic background” contribution to the  $D^* - D$  mass splitting as obtained from the ladder-rainbow DSE model and from the CQM model. They are fitted to the lattice data for comparison purposes.

error is 14%, while at the D meson the error is 30% [9].] The heavy quark limit of the relation produces [10]  $m_P \propto m_Q$  in accord with constituent quark behavior.

The current quark mass dependence of the DSE results for the ground state  $m_P$  and  $m_{P^*}$  has been studied recently [8, 9] with  $m_q$  fixed at  $m_u$  while  $m_Q$  varies in the range 0–300 MeV. The results are summarized well in terms of a single parameter  $\alpha$  by the forms

$$m_P^2 = \alpha_0 (m_q + m_Q) + \alpha^2 (m_q + m_Q)^2 \quad (6)$$

$$m_{P^*} = m_\rho + \alpha (m_q + m_Q - 2m_u) \quad , \quad (7)$$

where current quark masses are defined at a scale of  $\mu = 1$  GeV. The large  $m_q = m_Q$  behavior is consistent with recent DSE model studies [10, 18]. Here  $\alpha_0 = 1.724$  GeV is the DSE model-exact value of  $-\langle \bar{q}q \rangle_\mu^0 / (f_P^0)^2$ ; use of this term alone corresponds to the GMOR relation. The  $\alpha^2$  term accounts for the correction required by the exact pseudoscalar mass relation as reflected in the DSE results. The value  $\alpha = 1.079$  provides a good overall representation of the  $\pi/\rho, K/K^*, D/D^*$  and  $B/B^*$  meson masses. The absence of a linear term in Eq. (6) respects dynamical chiral symmetry breaking and this in turn provides a good representation of the increase in the physical hyperfine splittings with decreasing mass.

For any value of the parameter  $\alpha$ , the hyperfine splitting obtained from Eqs. (6) and (7) in the form  $y_P^{\text{DSE}} = m_{P^*} - m_P$  becomes independent of  $m_Q$  as  $m_Q \rightarrow \infty$ . In that limit, heavy quark effective theory makes a more specific

statement, namely  $y_P \rightarrow 0$ . This can be satisfied with the special value

$$\alpha = \frac{m_\rho}{4m_u} \left\{ 1 - \sqrt{1 - \frac{4m_u \alpha_0}{m_\rho^2}} \right\} \quad , \quad (8)$$

which yields  $\alpha = 1.138$ . Since the employed DSE calculations are limited by  $m_Q \leq 300$  MeV, we prefer to use  $\alpha = 1.138$  as a way of incorporating large  $m_Q$  physics. The “analytic background” as deduced from the DSE model is thus fully proscribed in magnitude and  $m_\pi$  dependence. To make an initial assessment of this  $m_\pi$ -dependent background, in comparison to  $y_P^{\text{CQM}}$ , we fit the form

$$y_P^{\text{DSE}} = m_{P^*} - m_P + \Delta_P \quad , \quad (9)$$

to the lattice data with  $\Delta_P$  being a free constant. The results are shown in Figs. 1 and 2. The required shifts  $\Delta_D = -0.0244$  GeV and  $\Delta_B = -0.0218$  GeV perform a role which is later taken over by the  $m_\pi$ -dependent pion loop contributions. As we note later, the pion loop contribution in the vicinity of the lattice data is indeed negative and of this order.

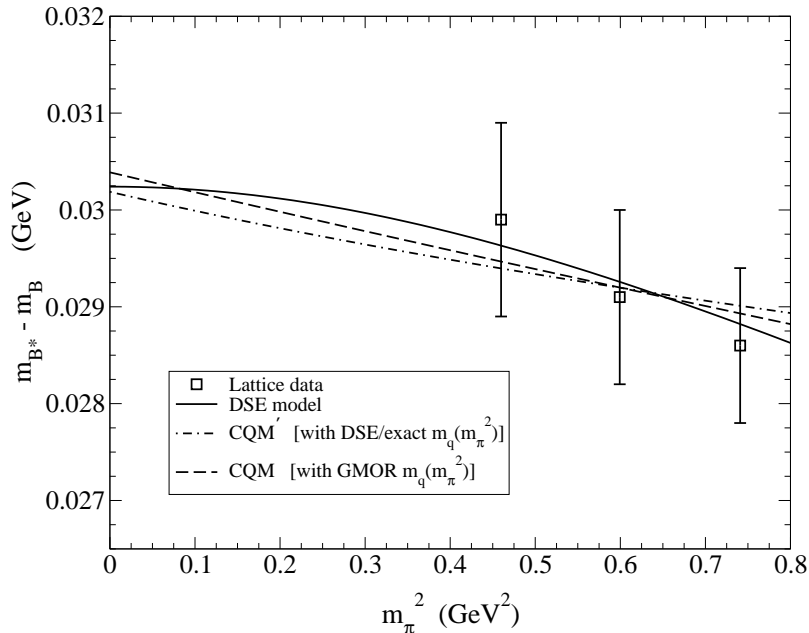


**Figure 2.** The “analytic background” contribution to the  $B^* - B$  mass splitting as obtained from the ladder-rainbow DSE model and from the CQM model. They are fitted to the lattice data for comparison purposes.

We note that the conversion of  $m_q$ -dependence into  $m_\pi$ -dependence, consistently within the DSE, has required the inversion of Eq. (6) with  $m_Q = m_q$ . One may ask whether the resulting  $m_q^{\text{DSE}}(m_\pi^2)$  differs sufficiently from the GMOR result  $m_q^{\text{GMOR}}(m_\pi^2)$  to warrant concern for the sensitive hyperfine splittings considered here. We provide information on this in Figs. 1 and 2 by means of two versions of the  $y_P^{\text{CQM}}$  description of the background. The version labelled CQM

employs  $m_q^{\text{GMOR}}(m_\pi^2)$ ; the version labelled CQM' employs  $m_q^{\text{DSE}}(m_\pi^2)$ . The results show this not to be a significant source of uncertainty; it amounts to a maximum of only 3 MeV in  $y_D$  at  $m_\pi = 0$ , and less for  $y_B$ . Uncertainties in the DSE description of the background from the parameterization in Eqs. (6) and (7) are not large. If we were to retain the parameter value  $\alpha = 1.079$  which is preferred by the low mass DSE calculations, the changes to the results shown in Figs. 1 and 2 are insignificant.

From Figs. 1 and 2 it is evident that there is more curvature in  $y_P^{\text{DSE}}$  than in  $y_P^{\text{CQM}}$ . This is due to the non-linearity imposed by chiral symmetry; the DSE model respects the axial vector Ward-Takahashi identity [7]. In Table 1 we summarize these representations of the ‘‘analytic background’’ in terms of would-be contributions to the hyperfine splittings at  $m_\pi = 0$ ; we also include the linear extrapolation results. The DSE model and the CQM are consistent with each other to about 5% and both tend to be slightly below the naive linear extrapolation. However, the linearly extrapolated splittings are already significantly too low: 15% low in the D meson case and 30% low for the B meson.

**Table 1.** Various background models extrapolated to  $m_\pi = 0$  and expressed as contributions to the hyperfine splitting. As explained in the text,  $m_q^{\text{GMOR}}(m_\pi^2)$  is used in CQM, while  $m_q^{\text{DSE}}(m_\pi^2)$  is used in CQM'. All quantities are in GeV units.

	CQM	CQM'	DSE	Linear	Expt
$y_D$	0.1224	0.120	0.1153	0.120	0.140
$y_B$	0.0304	0.0302	0.0303	0.032	0.046

## 4 Pion Loops

The pion loop contributions to the masses of heavy vector and heavy pseudoscalar mesons were calculated in Ref. [2]. The interaction between the pion and heavy mesons is generated from the following chiral Lagrangian for heavy mesons which is invariant under both chiral symmetry and heavy quark symmetry in the chiral and heavy quark limits, respectively [19]:

$$\mathcal{L} = -\text{Tr}[\bar{H}_a i v_\mu (D^\mu H)_a] + g \text{Tr}(\bar{H}_a H_b \gamma_\mu A_{ba}^\mu \gamma_5), \quad (10)$$

where  $D^\mu$  is the covariant derivative and  $A^\mu$  is the axial-vector field, both of which include Goldstone boson fields,  $g$  is the coupling constant describing the interactions between heavy mesons and Goldstone bosons, and  $H_a$  ( $a=1, 2, 3$  for  $u, d, s$  quarks, respectively) is a field operator which includes heavy pseudoscalar ( $P$ ) and heavy vector ( $P^*$ ) mesons:  $H_a = \frac{1+\not{v}}{2}(P_a^{*\mu} \gamma_\mu - P_a \gamma_5)$  ( $v$  is the velocity of the heavy meson). The correction term  $\frac{\lambda_2}{m_Q} \text{Tr} \bar{H}_a \sigma^{\mu\nu} H_a \sigma_{\mu\nu}$  was added to Eq. (10) (where  $\lambda_2$  is a parameter) since this term is responsible for hyperfine splittings. Based on experimental data we chose  $g^2$  to vary between 0.3 and 0.5 and  $\lambda_2$

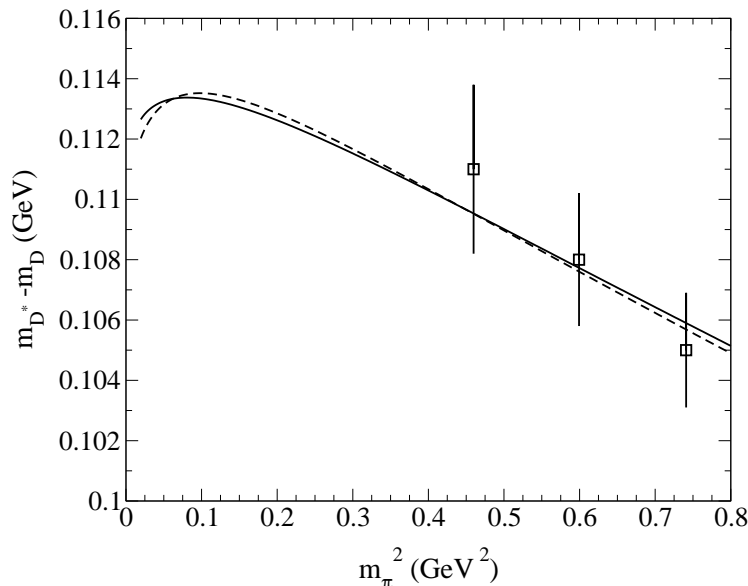


**Figure 3.** Extrapolation of the lattice data for the  $D^* - D$  hyperfine splitting using chiral loops, with a dipole form factor (solid line) and with a sharp-cutoff form factor (dashed line), added to the CQM model. The parameters are:  $\Lambda=0.4$  GeV,  $\lambda_2 = -0.015$  GeV<sup>2</sup>,  $g^2 = 0.4$  and  $e_D=6.9$  GeV<sup>2</sup>.

between  $-0.03$  GeV<sup>2</sup> and  $-0.02$  GeV<sup>2</sup> [2]. With Eq. (10)  $\bar{\sigma}_P$  can be expressed as the following:

$$\begin{aligned} \bar{\sigma}_P &= -\frac{g^2}{8\pi^2 f_\pi^2} \int_0^\infty dk \frac{k^4 u^2(k)}{\sqrt{k^2 + m_\pi^2}(\sqrt{k^2 + m_\pi^2} - \Delta)} \\ &- \frac{g^2}{4\pi^2 f_\pi^2} \int_0^\infty dk \frac{k^4 u^2(k)}{k^2 + m_\pi^2} \\ &+ \frac{3g^2}{8\pi^2 f_\pi^2} \int_0^\infty dk \frac{k^4 u^2(k)}{\sqrt{k^2 + m_\pi^2}(\sqrt{k^2 + m_\pi^2} + \Delta)}, \end{aligned} \quad (11)$$

where  $f_\pi = 132$  MeV is the pion decay constant,  $\Delta = -8\lambda_2/m_Q$ ,  $k$  is the absolute value of the three-momentum of the pion in the loop, and  $u(k)$  is an ultra-violet regulator. Since the leading nonanalytic contribution of pion loops is only associated with the infrared behavior of the integrals in Eq. (11), it does not depend on the details of the regulator. In this work we choose two different forms for the regulator. One is the sharp-cutoff,  $\theta(\Lambda - k)$ , and the other the dipole form, which is more realistic,  $\Lambda^4/(\Lambda^2 + k^2)^2$ . Here  $\Lambda$  characterizes the finite size of the source of the pion - i.e, the heavy meson's radius. In the fit we let  $\Lambda$  vary between  $0.4$  GeV and  $0.6$  GeV as in our previous work.

The hyperfine splittings for  $D$  and  $B$  mesons were calculated in Ref. [1], where NRQCD was used to treat the heavy quarks. For the bare gauge coupling  $\beta = 5.7$ , the inverse lattice spacing  $a^{-1}$  is about  $1.116$  GeV. The box size is  $2.1$  fm, corresponding to the volume  $12^3 \times 24$ . In their simulations, three different values for the hopping parameter  $\kappa$ ,  $0.1380$ ,  $0.1390$ , and  $0.1400$ , were used. The



light quark mass is related to  $\kappa$  as  $m_q = \frac{1}{2a}(1/\kappa - 1/\kappa_c)$ , with  $\kappa_c = 0.1434$ .

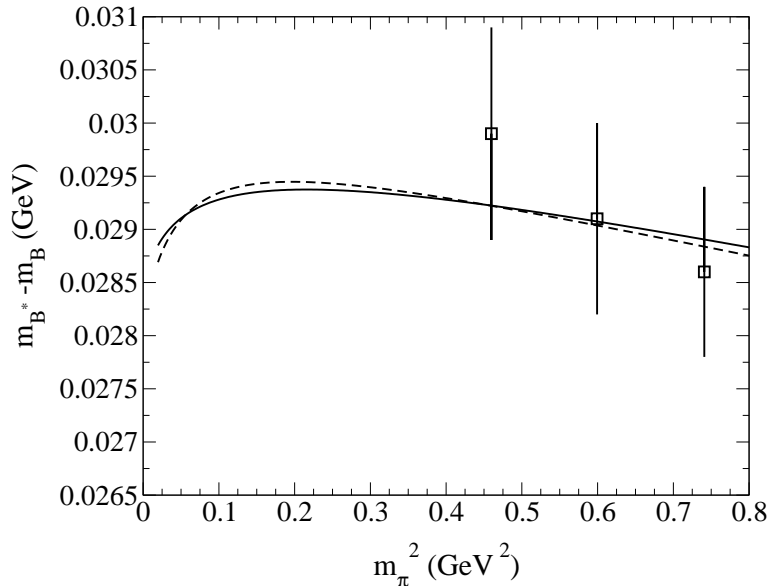


**Figure 4.** Extrapolation of the lattice data for the  $B^* - B$  hyperfine splitting using chiral loops, with a dipole form factor (solid line) and with a sharp-cutoff form factor (dashed line), added to the CQM model. The parameters are the same as those in Fig. 3 except that  $e_B=17.9$  GeV<sup>2</sup>.

The next step is to fit these lattice data with the form of Eq. (12) to determine the parameter  $d$ . The formulas in Eq. (11) are obtained in the infinite volume limit. Since the lattice simulations are performed on a finite volume grid, the finite size effects should be taken into account. Following the second reference in Ref. [4] and Ref. [20] we replace the continuum self-energy integral in Eq. (11) by a sum over the discrete pion momenta which are allowed on the lattice:  $\int d^3k \approx \left(\frac{2\pi}{aL}\right)^3 \sum_{k_x, k_y, k_z}$ , where the discrete momenta  $k_x, k_y, k_z$  are given by  $\frac{2\pi n}{aL}$ ,  $L$  is the number of lattice sites in each spatial direction, and the integer  $n$  satisfies the constraint  $-\frac{L}{2} < n \leq \frac{L}{2}$ . With  $1/a = 1.116$  GeV and  $L = 12$ , the smallest momentum allowed on the lattice,  $2\pi/aL$ , equals 0.58 GeV.

With the least square fitting method we fix the parameter  $d_P$  for different values of  $e_P$ ,  $\Lambda$ ,  $g$ , and  $\lambda_2$  in both the sharp-cutoff and the dipole schemes. It is noted that when  $m_\pi^2 \leq \Delta^2$  there is a pole in the first integral in Eq. (11). In this case, we have kept the principal value of the integral which is real. The difference between the integral and its principal value is imaginary and corresponds to the width of the heavy meson.

## 5 Results for Chiral Extrapolation

Based on the above considerations, we extrapolate the lattice data with the form

$$y_P = \bar{\sigma}_P + \frac{d_P}{e_P + m_\pi^2} \quad . \quad (12)$$

$d_P$  is a free parameter while, from Sec. 2, we constrain  $e_P$  to be within  $e_D \sim 5.5 - 8.2 \text{ GeV}^2$  and  $e_B \sim 16.5 - 19.2 \text{ GeV}^2$ . This direct extrapolation of the hyperfine splitting should lead to smaller errors than the separate extrapolation of masses carried out in Ref. [2].

For  $\bar{\sigma}_P$ , the allowed ranges of the parameters  $\Lambda$ ,  $g$ , and  $\lambda_2$  are those described in Sec 4. In Figs. 3 and 4 we show the fits to the lattice data for  $\Lambda = 0.4 \text{ GeV}$  and for the intermediate values of other parameters in both the dipole and the sharp-cutoff regulator schemes. When  $m_\pi < 500 \text{ MeV}$  the extrapolations start to deviate significantly from the constituent quark model. We require the fits to be within the uncertainties of the lattice data; this is always possible for  $\Lambda = 0.4 \text{ GeV}$  but not for  $\Lambda = 0.5 \text{ GeV}$  or  $0.6 \text{ GeV}$ <sup>1</sup>. In Table 2 the hyperfine splittings  $y_P$ , extrapolated to the physical pion mass, are listed as a range of values allowed by the variation of parameters as described above. We also give separately the relative uncertainties  $\Delta y/y$  caused by the errors in the lattice data. To assess the influence from the description of the background, we show results from use of the CQM background, Eq. (12), and from the linear background used in previous work, Eq. (1). The associated parameters are given in the Table.

**Table 2.** The hyperfine splittings extrapolated to the physical pion mass through chiral loops added to the background described via the CQM (with parameter  $d_P$ ) or the linear representation (with parameters  $a_P$  and  $b_P$ ). Results arising from the dipole form factor and the sharp-cutoff form factor are shown. The splittings  $y_P$  are shown as a range of values allowed by the variation of parameters as discussed in the text. Separately given are the relative uncertainties  $\Delta y/y$  caused by the errors in the lattice data.

	D Mesons		B Mesons	
Expt (GeV)	0.140		0.046	
Form Factor	Dipole	Sharp	Dipole	Sharp
With CQM background				
$y_P$ (GeV)	0.0983-0.1150	0.0978-0.1143	0.0260-0.0289	0.0259-0.0288
$d_P$ (GeV <sup>3</sup> )	0.6675-1.0601	0.6590-1.0237	0.5048-0.6467	0.4982-0.6245
$\Delta y/y$ (%)	1.24-1.45	1.25-1.46	1.82-2.02	1.83-2.03
With Linear background				
$y_P$ (GeV)	0.1000-0.1162	0.0965-0.1149	0.0270-0.0309	0.0256-0.0306
$a_P$ (GeV)	0.1226-0.1395	0.1203-0.1375	0.0326-0.0374	0.0320-0.0369
$-b_P$ (GeV <sup>-1</sup> )	0.0308-0.0216	0.0340-0.0203	0.0077-0.0051	0.0086-0.0047
$\Delta y/y$ (%)	6.28-7.30	6.36-7.57	8.90-10.18	9.00-10.76

With our parameter ranges, the extrapolated hyperfine splitting with CQM background for  $D$  mesons varies from 0.0983 GeV to 0.115 GeV with the dipole

<sup>1</sup>When the fit results are not required to be within the lattice uncertainties the high limiting values of  $y_P$  remain unchanged while the low limiting values are reduced by about 8~17%. The values of the parameters  $d_P$ ,  $a_P$ , and  $b_P$  are not affected.

form factor, and from 0.0978 GeV to 0.114 GeV with the sharp-cutoff form factor. For  $B$  mesons, it varies from 0.0260 GeV to 0.0289 GeV and from 0.0259 GeV to 0.0288 GeV, respectively. On the other hand, with use of the linear background the  $D$  meson result is in the range 0.100-0.116 GeV from the dipole form factor, and in the range 0.0965-0.115 GeV from the sharp-cutoff form factor. For  $B$  mesons, the extrapolated hyperfine splittings are 0.0270-0.0309 GeV and 0.0256-0.0306 GeV, respectively. The largest extrapolated hyperfine splittings we could obtain are about 115 MeV and 29 MeV for  $D$  and  $B$  mesons, respectively from the CQM background; with the linear background, these become 116 MeV and 31 MeV, respectively. The present approach is unable to do better than 17% below experiment for the  $D$  splitting and 35% below experiment for the  $B$  splitting. These are further from experiment than the naive linear extrapolation which, as described in Sec. 3, produces a  $D$  splitting 15% below and a  $B$  splitting 30% below.

One can compare the values at the midpoints of the ranges of the CQM background parameters  $e_P$  and  $d_P$  that fit the lattice data in the presence of the pion loop contribution, to the corresponding values obtained in Sec. 2 by the fit of the CQM background alone to the data. This confirms that at  $m_\pi^2 \approx 0.6 \text{ GeV}^2$  the pion loop contribution to  $y_D$  is typically  $-10 \text{ MeV}$ , and the contribution to  $y_B$  is typically  $-20 \text{ MeV}$ . These values are of the same order as the typical shifts  $\Delta_D$  and  $\Delta_B$  found in Sec. 3 to align the DSE background with the lattice data.

In addition to the uncertainties which are associated with the parameters  $\lambda_2$ ,  $g$ ,  $\Lambda$ , and  $e_P$  we also analysed the uncertainties which are caused by the errors in the lattice data. As expected, these uncertainties are much smaller (less than 2%) with the improved CQM background description compared to the linear treatment of the background (6~11%). Taking into account such uncertainties, we can see that the ranges of the extrapolated hyperfine splittings produced with the different background treatments are compatible with each other.

Another interesting quantity is the slope of the fit line at large  $m_\pi$ . From Figs. 3 and 4 we can see that the slope of the fit for  $B$  mesons is much smaller than that for  $D$  mesons. The CQM representation of the background carries a  $1/M_Q^2$  dependence for the slope and provides a natural fit. In contrast, the linear representation of the background contains no  $M_Q$  dependence and this contributes to the larger uncertainties that result. The difference of slopes in these two extrapolation forms could be tested with more accurate lattice data.

In the above fit we have treated the lattice data as truly statistical. Since the lattice data are highly correlated we could also fit the top and the bottom of the three data points in Figs. 3 and 4 to give the ranges of the fit. This may lead to a little change in the results. As an example, we consider the largest extrapolated hyperfine splittings for  $D$  and  $B$  mesons in Figures 3 and 4. If we fit the top of the three lattice data in these two figures in the dipole scheme we obtain the extrapolated results as 0.1177 GeV and 0.0299 GeV for  $D$  and  $B$  mesons, respectively. These values are a little bigger than those obtained when we treat the lattice data as truly statistical.

## 6 Summary

We have explored a number of issues that arise in the chiral extrapolation of the lattice data for hyperfine splittings of  $D$  and  $B$  mesons from the domain of large mass of the light quark to the physical point. We improve on previous work by investigating the description of the non-chiral background via both the constituent quark model (CQM) and the modeling of QCD via the Dyson Schwinger equations (DSEs) in ladder-rainbow truncation. We find that these descriptions of the background are consistent with each other. Thus the form employed here for the analytic background for extrapolation in  $m_\pi^2$  is consistent with: chiral symmetry, heavy quark symmetry in the limit of infinite heavy quark mass, the constituent quark model, and the DSE modeling of QCD. We adopt the CQM background, add the difference of the chiral loop self-energies for vector and pseudoscalar mesons, and fit to the lattice data. We extract a range of extrapolated hyperfine splittings at the physical pion mass for both  $D$  and  $B$  mesons, as allowed by the theoretical uncertainties in parameters and pion-baryon form factors.

In comparison to our previous work [2, 3] that employed an analytic background linear in  $m_\pi^2$ , the present approach has a better physical basis in the dependence of the background upon both  $M_Q$  and  $m_\pi^2$ . The pion-loop contribution  $\bar{\sigma}_P$  produces essentially all of the curvature evident in Figs. 3 and 4 at low  $m_\pi^2$  and this is clearly less curvature than what we obtained in Ref. [2]. This is because the present approach deals directly with the hyperfine splitting and its extrapolation. There is a single form factor range  $\Lambda$  for a vector-pseudoscalar meson pair. In contrast, the previous work [2] dealt with extrapolation of the meson masses separately before the difference is formed. That procedure employed separate form factor parameters  $\Lambda$  for each meson and the resulting splittings were a difference of two quantities having different curvatures at low  $m_\pi^2$ . The present more direct procedure has less curvature as a result of being better constrained by physics. It has smaller uncertainties in the extrapolated splittings from errors in the lattice data. We conclude that the present procedure is more reliable.

In contrast to extrapolations of lattice data for hadron masses [21] and magnetic moments [22], the 1-loop chiral loop self-energies do not improve the agreement of the extrapolated results for hyperfine splittings in comparison with experiment. This work has explored the analytic background carefully and we conclude that this is not a likely explanation. Although sub-leading nonanalytic behavior from higher order chiral loops could be examined, we conclude that more reliable lattice simulations for hyperfine splittings are required to resolve this situation. One would like to have data for full QCD, so as to not rely on the quenched approximation. The experimental mass splittings are small: 7% for  $D$  mesons and 0.8% for  $B$  mesons. The  $\sigma \cdot \mathbf{B}$  term in NRQCD is of order  $1/M_Q$  and small corrections can have a magnified impact. The coefficient of this term may well be increased by the inclusion of radiative corrections beyond tadpole improvement, the possible light quark mass dependence of the clover coefficient in the clover action for light quarks, and higher order terms in NRQCD. With the physical improvements incorporated here, the extrapolation is unable to do better than 17% below experiment for the  $D$  splitting and 35% below experi-

ment for the  $B$  splitting. These are further from experiment than the naive linear extrapolation which produces a  $D$  splitting 15% below and a  $B$  splitting 30% below. The fact that the deviation from experiment for  $B$  splitting is consistently double that for  $D$  splitting is suggestive of systematic errors in the lattice data. Higher quality lattice data would stimulate greater theoretical scrutiny of both analytic and nonanalytic behavior in  $m_\pi^2$  for such a sensitive quantity.

*Acknowledgement.* Craig Roberts is acknowledged for helpful conversations. This work was supported by the Australian Research Council, by NSF grants No. PHY-0071361, INT-0129236, and PHY-0301190, by DOE contract DE-AC05-84ER40150, under which SURA operates Jefferson Lab, and by the Special Grants for "Jing Shi Scholar" of Beijing Normal University.

## References

1. Hein, J. *et al.*: Phys. Rev. **D62**, 074503 (2000).
2. Guo, X.-H. and Thomas, A. W.: Phys. Rev. **D65**, 074019 (2002).
3. Guo, X.-H. and Thomas, A. W.: Phys. Rev. **D67**, 074005 (2003).
4. Leinweber, D. B., Thomas, A. W., Tsushima, K., and Wright, S. V.: Phys. Rev. **D61**, 074502 (2000); Phys. Rev. **D64**, 094502 (2001); Hackett-Jones, E. J., Leinweber, D. B., and Thomas, A. W.: Phys. Lett. **B489**, 143 (2000); Leinweber, D. B. and Thomas, A. W.: Phys. Rev. **D62**, 074505 (2000); Detmold, W., Melnitchouk, W., and Thomas, A. W.: Eur. Phys. J. **C13**, 1 (2001); Detmold, W., Melnitchouk, W., Negele, J. W., Renner, D. B., and Thomas, A. W.: Phys. Rev. Lett. **87**, 172001 (2001); Hackett-Jones, E. J., Leinweber, D. B., and Thomas, A. W.: Phys. Lett. **B494**, 89 (2000).
5. Roberts, C. D. and Williams, A. G.: Prog. Part. Nucl. Phys. **33**, 477 (1994)
6. Cloet, I. C., Leinweber, D. B., and Thomas, A. W.: Phys. Rev. **C65**, 062201(R) (2002).
7. Maris, P., Roberts, C. D., and Tandy, P. C.: Phys. Lett. **B420**, 267 (1998).
8. Maris, P.: arXiv:nucl-th/0009064.
9. Tandy, P. C.: Prog. Part. Nucl. Phys. **50**, 305 (2003).
10. Ivanov, M. A., Kalinovsky, Y. L., and Roberts, C. D.: Phys. Rev. **D60**, 034018 (1999).
11. Lucha, W., Schoberl, F. F., and Gromes, D.: Phys. Rept. **200**, 127 (1991).
12. Isgur, N. and Wise, M. B.: Phys. Lett. **B232**, 113 (1989); **B237**, 527 (1990); Georgi, H.: Phys. Lett. **B264**, 447 (1991); see also Neubert, M.: Phys. Rep. **245**, 259 (1994) for a review.
13. Maris, P. and Roberts, C. D.: Phys. Rev. **C56**, 3369 (1997).
14. Maris, P. and Tandy, P. C.: Phys. Rev. **C60**, 055214 (1999).

15. Maris, P. and Tandy, P. C.: Phys. Rev. **C62**, 055204 (2000).
16. Maris, P. and Tandy, P. C.: Phys. Rev. **C65**, 045211 (2002).
17. Ji, C. R. and Maris, P.: Phys. Rev. **D64**, 014032 (2001).
18. Bhagwat, M. S., Holl, A., Krassnigg, A., Roberts, C. D., and Tandy, P. C.: Phys. Rev. **C70**, 035205, (2004).
19. Wise, M. B.: Phys. Rev. **D45**, R2188 (1992).
20. Young, R. D., Leinweber, D. B., Thomas, A. W., and Wright, S. V.: Phys. Rev. **D66**, 094507 (2002).
21. Leinweber, D. B., Thomas, A. W., and Young, R. D.: Phys. Rev. Lett. **92**, 242002 (2004).
22. Leinweber, D. B., Lu, D. H., and Thomas, A. W.: Phys. Rev. **D60**, 034014 (1999).

First received October 2005; accepted in final form Month, day, year.